Recovering the degeneracy in quasi two-dimensional artificial colloidal ice

Author: Oriol Raba Parodi.
Tutors: Antonio Ortiz-Ambriz & Pietro Tierno.
Facultat de Física, Universitat de Barcelona, Diagonal 645, 08028 Barcelona, Spain.

Abstract: Artificial Spin Ice systems have been used to investigate exotic behaviours of frustrated systems. In this project, I study geometric frustration through computer simulations of Artificial Colloidal Ice which is made of an ensemble of magnetized colloids confined in bistable traps and arranged to form a square lattice. By implementing an offset height between perpendicular traps, it is possible to recover a degenerate ground state in the system.

I. INTRODUCTION

Geometric frustration in particle systems is the inability to minimize all local energies simultaneously due to certain topological constraints on the system [1]. This behaviour is usually originated from atomic interactions which compete on a regular structure. Geometrically frustrated systems are often found to have degenerate low energy states at very low temperatures, in addition to having a non-zero entropy, also called residual entropy. The residual entropy found in frustrated systems was first investigated on water ice by Linus Pauling in 1935 [2]. Water ice is made up of oxygen atoms with two hydrogen atoms in covalent bonds. At low temperatures, hydrogen atoms can move between the fixed oxygen atoms due to atomic interactions and form covalent bonds with one of the four first neighbouring oxygen atoms. But water ice has the topological restriction that each oxygen requires two hydrogen atoms linked via covalent bonds, then the hydrogen atoms are rearranged to comply with the constraint. The different distributions of hydrogen atoms in ice at low temperatures produce the residual entropy along with a degenerate ground state. This topological constraint found in water ice is called ice rule, and it is an important feature highly used in the creation of ice-like artificial systems. [3]
Currently, several natural materials show geometric frustration, such as spin glasses [4], or spin ice [5]. These materials are magnetic systems that behave similarly to ice at low temperatures, presenting a residual entropy. Spin ice also fulfills the same topological constraint called ice rule. [5]
The recent discovery of numerous spin ice materials such as rare earth pyrochlore oxides $Dy_2Ti_2O_7$ and $Ho_2Ti_2O_7$ [5], has motivated the creation of artificial systems, such as Artificial Spin Ice (ASI) [6] and Artificial Colloidal Ice (ACI) [7], with the objective of replicating the behaviors found in these materials and studying their emergent exotic properties.
These systems are created by making a two-dimensional projection of real spin ice materials, so that the particles are fixed on a two-dimensional (2D) lattice. To observe geometric frustration the colloidal systems use magnetized particles, restraining its movement through traps that act as topological constraints. The traps are arranged to form different lattices depending on the design of the system, for example there is the triangular lattice, square lattice and hexagonal lattice. The main advantage of creating Artificial Colloidal Ice systems is the ability to observe the individual particles via optical microscopy, and control them via external fields in a much higher temperature range than the real materials while still showing frustrated behaviours. [8]
Artificial Spin Ice systems are created using magnetic dipoles as particles and magnetic nano-islands as traps. The direction in which the spin points would be analogous to the position a hydrogen atom is between two oxygen atoms in water ice. Differently, Artificial Colloidal Ice systems are created using bistable traps that contain magnetized colloids. Due to magnetic dipolar interactions and thermal effects, colloids can move within the trap jumping from one stable point to the other. The position of the colloid in the trap would be analogous to the position a hydrogen atom is between two oxygen atoms on water ice. [8]
Colloidal systems have an experimental advantage over spin systems due to less complexity in observing the experiment, since the ASI has a nanometric scale while the colloidal system is characterized by a micrometric scale. The colloids are placed in lithographic traps within a fluid of lower density using optical tweezers, once each colloid is in a trap, a magnetic field is applied perpendicular to the plane of the traps. The field induces dipole moments within the particles, and as a result there is an isotropic repulsive interaction between particles. This interacting force can be modulated by tuning the amplitude of the applied magnetic field. [9]

II. METHODOLOGY

In this project, simulations of 3D Brownian dynamics of magnetized colloids trapped in bistable traps have been performed using the open-source code of classical molecular dynamics LAMMPS [10]. The traps and colloids are submerged in a low viscosity fluid and are arranged forming a three-dimensional square lattice as shown in Figure 1 a) and b), where the traps parallel to the y axis are at an offset height relative to the traps parallel to the x axis.
Each of the colloids movement has been calculated using the equations of motion given by Newton's second law

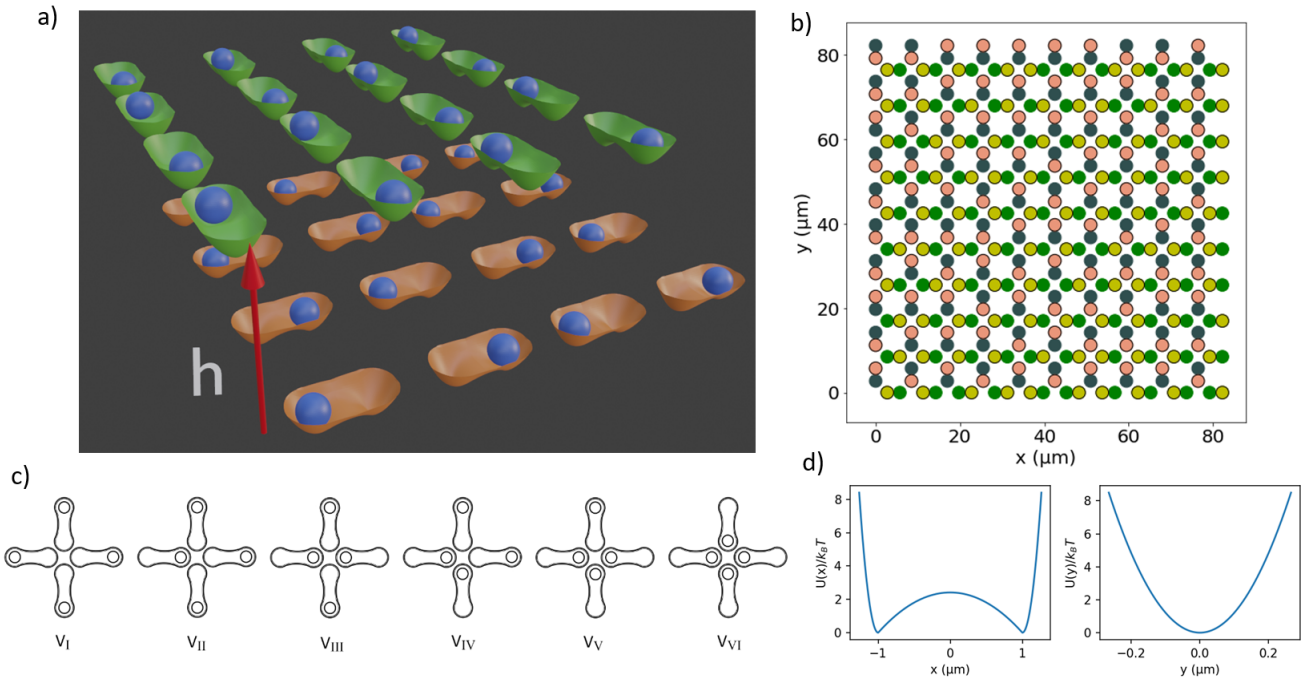

FIG. 1: **a)** Three-dimensional representation of the system used in the simulations. The traps are separated by a height h. **b)** Graph showing a zenith view of the system for a 3 μm colloid square lattice. The colors of the trap indicate the difference in height, in addition to showing the direction of the colloid relative to the center of the trap. Colloids are displayed with black outlines. **c)** Qualitative description of each vertex type in a square lattice. **d)** Graphical representation of the trap potential relative to the x and y axis.

$m_i\ddot{x}_i = \vec{F}_i$. There is a drag force produced by the viscosity of the fluid $F_i^\gamma = -\gamma\dot{x}_i$, which is assumed to be much larger than the inertial term $m_i\ddot{x}_i$. Then, by doing the sum of forces, the overdamped equation of motion for a colloid i is:

$$\eta\frac{dr_i}{dt} = F_i^{cc} + F_i^T + F_i^G + F_i^{th}$$

where the damping constant is $\eta = 1.0$. The colloid-colloid interaction F_i^{cc} is a dipole interaction. The force applied to one colloid is the sum of the interaction force of this particle with the rest. This two-body interaction is given by the force between two magnetic dipoles separated by a distance r:

$$F(\vec{r},\vec{m_1},\vec{m_2}) = \frac{3\mu_0}{4\pi r^5}[(\vec{m_1}\cdot\vec{r})\vec{m_2} + (\vec{m_2}\cdot\vec{r})\vec{m_1} + \\ + (\vec{m_1}\cdot\vec{m_2})\vec{r} - \frac{5(\vec{m_1}\cdot\vec{r})(\vec{m_2}\cdot\vec{r})}{r^2}\vec{r}] \quad (1)$$

In the previous equation, $\vec{r}$ represents the distance between two colloids, $\vec{m_i}$ is the magnetic moment of a colloid: $\vec{m} = \frac{1}{\mu_0}V\chi_0\vec{B_{ext}}$, where $\vec{B_{ext}}$ is the applied magnetic field which is perpendicular to the XY plane, $V = \frac{4\pi}{3}r^3$ is the colloid volume with r its radius, χ_0 is the magnetic susceptibility and μ_0 is the permeability of vacuum. All colloids must have the same magnetic moment since the external magnetic field is constant throughout the whole volume. If all colloids were in the same plane, equation (1) would be shortened to: $F(\vec{r},\vec{m_1},\vec{m_2}) = \frac{3\mu_0}{4\pi r^5}[(\vec{m_1}\cdot\vec{m_2})\vec{r}]$.

The force applied by the traps F_i^T is calculated from the potential shown in Figure 1 d), defined by:

$$F = -kr_\perp\hat{e}_\perp + \hat{e}_\parallel\begin{cases}k(r_\parallel - d/2)sgn(r_\parallel) & r_\parallel < d/2\\ hr_\parallel & r_\parallel > d/2\end{cases} \quad (2)$$

where $r_\parallel$ is the component parallel to the direction of the trap with $\hat{e}_\parallel$ its unit vector, $r_\perp$ is the perpendicular component with $\hat{e}_\perp$ its unit vector, k is the trap stiffness, d is the distance between the two stable points, and h is the stiffness of the central hill. This represents a parabolic potential with a barrier between the stability points, with a maximum height that can be modulated.
The gravitational force F_i^G limits the colloid movement on the z axis, and is given by the buoyancy equation: $F_i^G = Vg(\rho_c - \rho_f)$, where V and ρ_c are the colloids volume and density, g is gravity and ρ_f is the fluid density.
Thermal forces F_i^{th}, are given by a Gaussian random process based on the Langevin equation with mean $< F_i^{th} >= 0$, and correlation $< F_i^{th}(t)F_j^{th}(t') >= 2k_BT\eta\delta_{ij}\delta(t-t')$.

The simulations have been performed using two sets of parameters: one has a colloid radius of 5.15 μm, and will be referred as 10 μm colloids, with a susceptibility $\chi_0 = 0.06$ and a trap potential barrier of height $U = 60pN/nm$. The lattice constant for these particles is 30 μm and a trap separation of 10 μm. The second one has a colloid radius of 1.4 μm, and will be referred as 3 μm colloids,

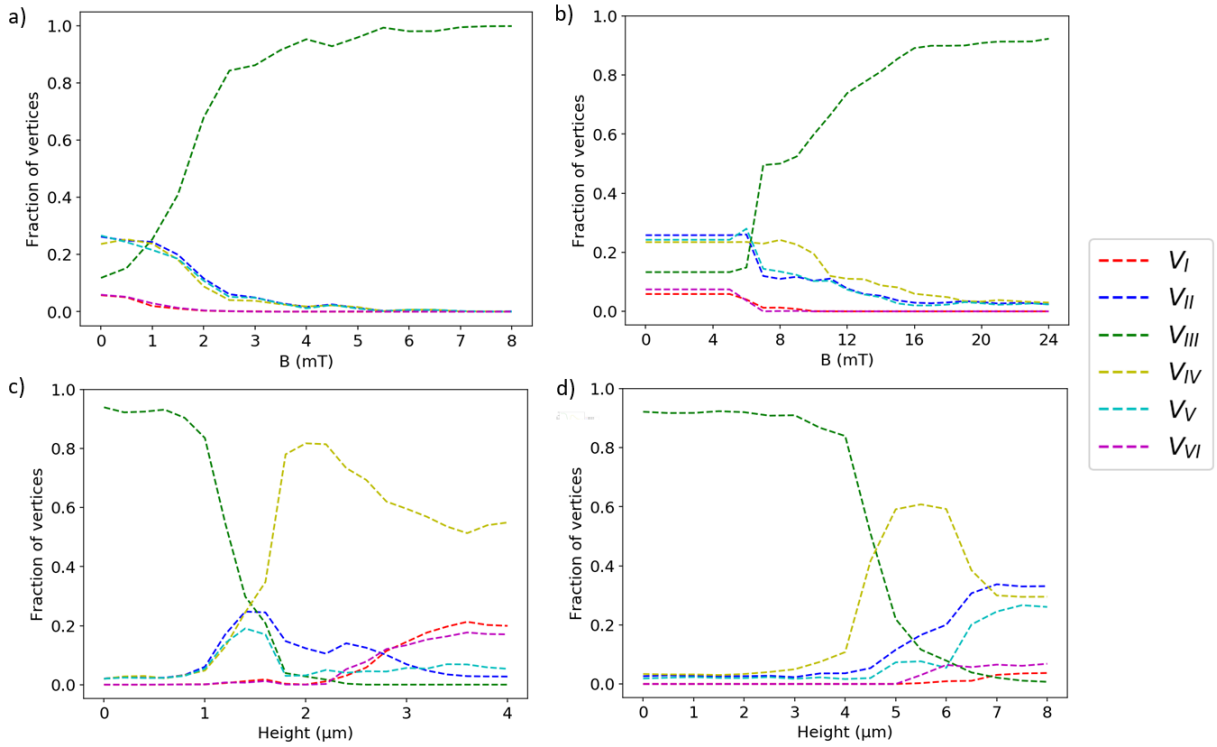

FIG. 2: Graphs showing the fraction of vertices in the system as a function of the applied magnetic field **a)** & **b)** and offset height **c)** & **d)**, for 3 μm particles **a)** & **c)** and 10 μm particles **b)** & **d)**.

with a susceptibility $\chi_0 = 0.4$ and a trap potential barrier of height $U = 4\, pN/nm$. The lattice constant for these particles is 8.4 μm with a trap gap of 3 μm. The values of the lattice constant and the separation between traps are calculated by setting the minimum distance between 2 traps to be 1 micrometer.
The values used for particle density and temperature are: $\rho = 1000\, kg/m^3$ and $T = 300\, K$. Most parameters are set to mimic the experiments (see [9]).
All simulations were carried out using a 20x20 vertex square lattice, which translates into a sum of 800 traps and 800 colloids where half of the particles can move along the x axis and the other half along the y axis. To eliminate boundary effects, vertices that are at the system boundaries have not been taken into account in the calculations. Furthermore, for each simulation the initial position of each colloid in a trap is one of the two stable points selected at random. All results are calculated by a mean of 10 seed iterations.

III. RESULTS

A. Field and height dependence

In Figure 2 a) and b) I show the output of simulations performed at zero offset height. By increasing the external magnetic field we increase the interaction force between particles. Since initially the particles are in random positions, we can see from Figure 2 b) that the initial vertex fraction remains unchanged from $B = 0 mT$ to $B = 5 mT$ due to the high potential barrier. At higher magnetic field values, we observe an increase in type 3 vertices while the rest of the vertices decrease until the system reaches a state where only type 3 vertices appear. Thus, for strong magnetic fields, the system tends to stabilize to a ground state.
By having a large potential barrier, thermal effects are negligible and we do not obtain spontaneous jumps between stability points by particles, opposite to what happens with low potential barriers.
In Figure 2 a) we see that when the magnetic field $B^{gs} = 5\, mT$, the system has already stabilized the ground state. Analogously, in Figure 2 b) we find $B^{gs} = 20\, mT$.

In Figure 2 c) and d) I show the output of simulations performed at different offset heights, and constant magnetic field B^{gs}. By increasing the height we are modifying the interaction force between the colloids. At small offset heights, the forces are dominated by the dot product of magnetic moments in equation (1), as we increase the offset height the magnitude of other components also increase.
From both graphs we observe that as we increase the height offset, the fraction of type 3 vertices decreases while the other vertices increase, especially type 4. We obtain a balance between type 3 and type 4

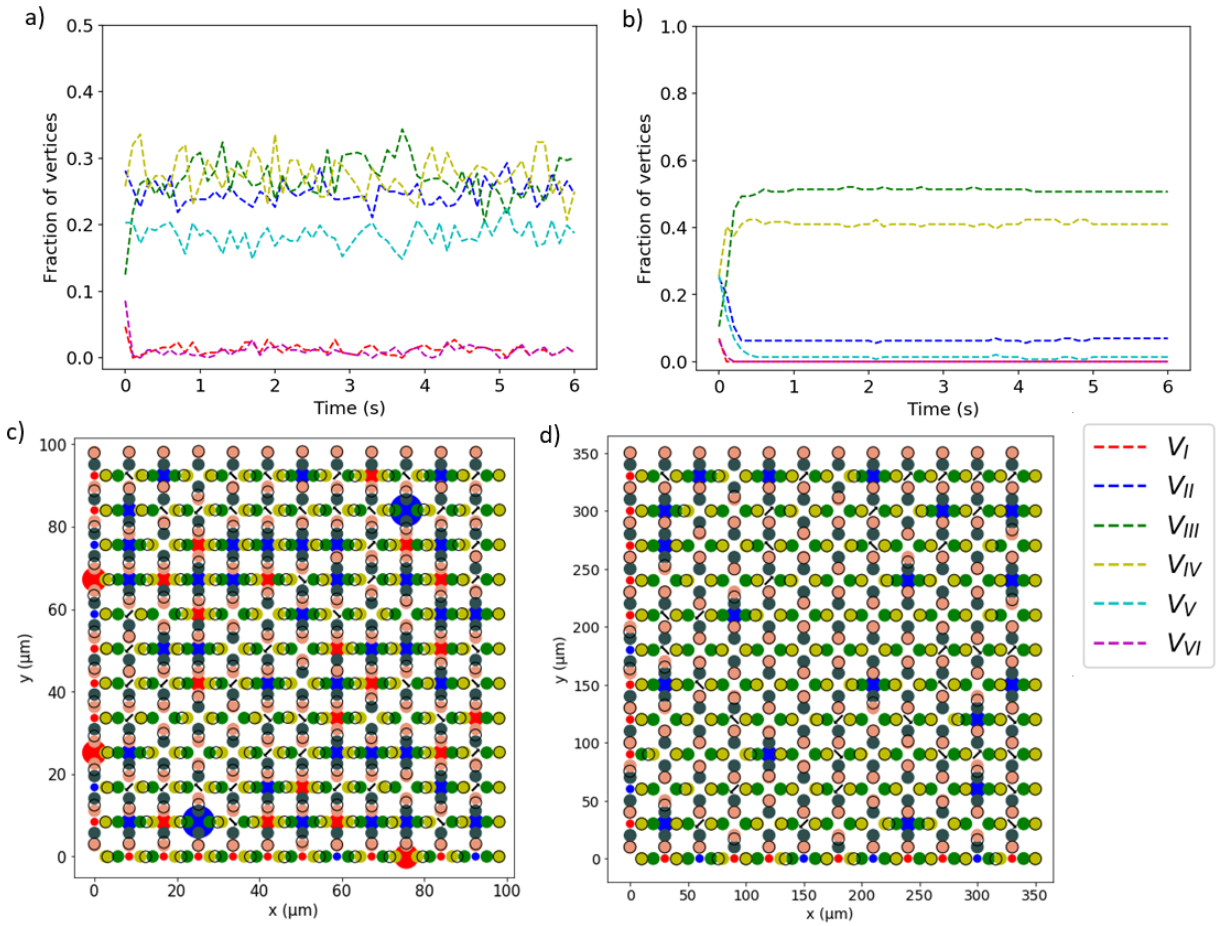

FIG. 3: Both **a)** & **b)** graphs show the evolution in time of vertex fractions **a)** for 3 μm colloids and **b)** for 10 μm colloids, under a constant field B^{gs} and a constant height h^{deg}. Both **c)** & **d)** graphs show a lattice at the degenerate height for 3 μm colloids **c)** and 10 μm colloids **d)**. Type 4 vertices are displayed by an arrow and types 2 & 5 are displayed by red and blue circles respectively.

vertices at the height at which their lines intersect, also called degenerate height. This degenerate height is $h^{deg} = 4.45 \pm 0.05\ \mu m$ for 10 μm colloids and $h^{deg} = 1.45 \pm 0.05\ \mu m$ for 3 μm colloids.

B. Behaviours at the degenerate height

In Figure 3 a) and c) there is an instability with a big exchange of vertices each second, given mainly by thermal effects and the interacting forces reacting to these changes. In Figure 3 b) and d), the thermal force is not relevant in the system, therefore, the vertex fraction is constant over time. For values of offset height other than the degenerate height, we obtain a behavior identical to Figure 3 b) in which the fraction of each vertex is stabilized, this happens due to the dependence of the interacting forces with height.
In Figure 3 d) we see that at the degenerate height for 10 μm colloids, most of the particles are in one of the stable points of the traps, while at the degenerate height shown in Figure 3 c), most of the colloids are in a position between the stable points due to low barrier height. Then, degeneracy is only recovered at a degenerate height when thermal forces are relevant in the system.

C. Correlations

Lastly, we can obtain the system correlations by calculating the radial correlation function:
$g(r'-r) =< C_i(r,t) \cdot C_j(r',t) >$, where C_i is a colloids position vector relative to the center of its trap, $(r'-r)$ is the distance between the centers of each pair of traps. This correlation function is similar to a two-dimensional square Ising model, but instead of spin values, correlations are calculated through position vectors. The main difference with the calculations is that it involves a dot product between two three-dimensional vectors. Since colloids mainly move along one axis and half of the colloids motion axis is perpendicular to the other half, correlations between them are almost null when they are found at one of the stable points of their trap.
Since colloids are arranged in a square lattice, the dis-

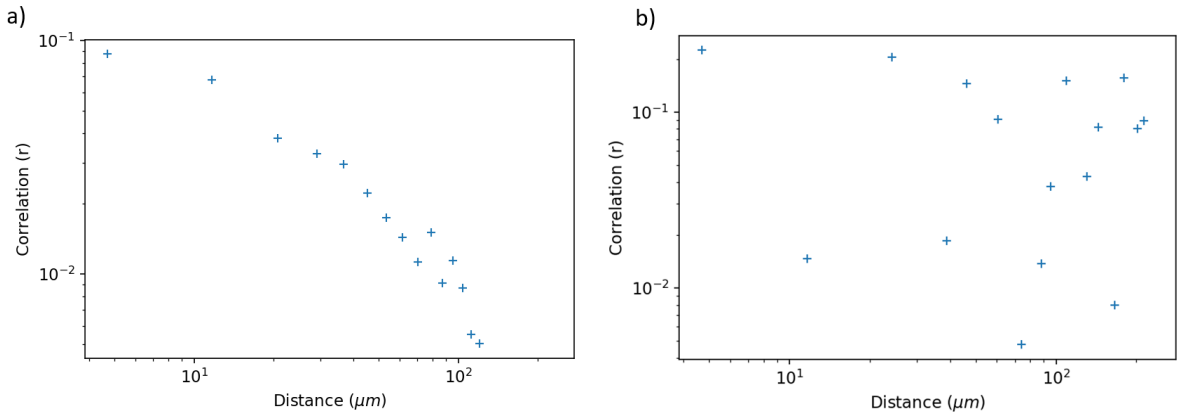

FIG. 4: Double logarithmic graph of the correlation function for 3 μm colloids at a degenerate height $h = 1.45\,\mu m$ **a)** and at a non-degenerate height $h = 0\,\mu m$ **b)**. Data points represent a mean of the correlations between discrete radial positions.

tance between colloids is discrete, therefore I make calculations of g(r) by doing a mean of correlations for small increments of r.
In Figure 4 a) we can see an almost constant correlation decay until the distance reaches a half of the system size, where the correlation decays rapidly with distance. In Figure 4 b), the decay is not well defined since the system is at the ground state and most vertices are type 3. Since the ground state is a periodic distribution, almost every colloid sees the rest of the colloids at the same position, resulting in non constant correlation distribution.

IV. DISCUSSION AND FUTURE WORK

Using the results obtained, although the particles movement is restricted by traps, we can approximate a free movement throughout the entire system of all vertex types at the degenerate height. Then, these vertices could be studied as differentiated particles with an interaction energy between them, in addition to having a probability to exchange energy and having a continuous movement in the lattice. Observing the graphs of Figure 3 c), type 3 vertices could behave as points of stability that determine a minimum of interacting forces between vertices. This degenerate state could also be compared with the one obtained at a null offset height, and the differences between the systems properties could be researched.

V. CONCLUSIONS

In summary, we have studied the behavior of an artificial colloidal ice system trapped by bistable traps in a square lattice with an offset height. Initially, we found a degenerate state for weak magnetic fields until we found stability for strong fields. Then, modifying the height we could recover a degenerate state for a small range of heights, while at other heights there is equilibrium. Finally, we have verified the relevance of the thermal effects in a system to recover frustration at degenerate heights.

[1] Moessner, R. & Ramirez, A. P. Geometrical frustration. Phys. Today 59, 24–29 (2006).
[2] Pauling, Linus, 1935, "The structure and entropy of ice and of other crystals with some randomness of atomic arrangement", J. Am. Chem. Soc. 57, 2680–2684.
[3] Bernal, J. D., and R. E. Fowler, 1933, "theory of water and ionic solution, with particular refefence to H+ and OH- ions," J. Chem. Phys. 1, 515.
[4] Mydosh, John A., 2014, Spin glasses: an experimental introduction (CRC Press, Boca Raton).
[5] Bramwell, S. T., and M. J. P. Gingras, 2001, "Spin ice state in frustrated magnetic pyrochlore materials," Science 294, 1495–1501.
[6] Perrin, Yann, Benjamin Canals, and Nicolas Rougemaille, 2016, "Extensive degeneracy, Coulomb phase and magnetic monopoles in an artificial realization of the square ice model", Nature (London) 540, 410–413.
[7] Libál, A., C. Reichhardt, and C. J. Olson Reichhardt, 2006, "Realizing colloidal artificial ice on arrays of optical traps," Phys. Rev. Lett. 97, 228302.
[8] Ortiz-Ambriz, Antonio and Nisoli, Cristiano and Reichhardt, Charles and Reichhardt, Cynthia J. O. and Tierno, Pietro "Colloquium: Ice rule and emergent frustration in particle ice and beyond." Rev. Mod. Phys. doi: 10.1103/RevModPhys.91.041003.
[9] Ortiz-Ambriz, A. & Tierno, P. Engineering of frustration in colloidal artificial ices realized on microfeatured grooved lattices. Nat. Commun. 7:10575 doi: 10.1038/ncomms10575 (2016).
[10] https://lammps.sandia.gov.
S. Plimpton, Fast Parallel Algorithms for Short-Range Molecular Dynamics, J Comp Phys, 117, 1-19 (1995).